Research Square

Preprints are preliminary reports that have not undergone peer review.
They should not be considered conclusive, used to inform clinical practice,
or referenced by the media as validated information.

Peroxisomal fatty acid oxidation in rod photoreceptors regulates essential fatty acids for retinal visual function

Yan Zeng
Boston Children's Hospital
Chuck T. Chen
University of Toronto
Mengxu Ge
Boston Children's Hospital
Myriam Boeck
Boston Children's Hospital
Hitomi Yagi
Boston Children's Hospital
Hiroyuki Komatsu
Boston Children's Hospital
Emil Kriukov
Massachusetts Eye and Ear
Victoria Hirst
Boston Children's Hospital
Michelle Lee
Boston Children's Hospital
Katherine Neilsen
Boston Children's Hospital
Tommy S. Fong
University of Toronto
Yan Fu
University of Toronto
Joshua L. Dunaief
University of Pennsylvania
James D. Akula
Boston Children's Hospital
Petr Baranov
Massachusetts Eye and Ear
Jing Chen

Boston Children's Hospital

Irfan J. Lodhi
Washington University in St. Louis

Richard P. Bazinet
University of Toronto

Lois E.H. Smith
Boston Children's Hospital

Zhongjie Fu
zhongjie.fu@childrens.harvard.edu

Boston Children's Hospital

Short Report

Keywords: peroxisomal fatty acid oxidation, ACOX1, retinal lipid homeostasis, retinal DHA, retinal function

Posted Date: November 18th, 2026

DOI: https://doi.org/10.21203/rs.3.rs-11542330/v1

License: This work is licensed under a Creative Commons Attribution 4.0 International License.
Read Full License

Additional Declarations: Competing interest reported. JC serves as a consultant to EyePoint Pharmaceuticals. The authors have no other competing interests to declare.

Peroxisomal fatty acid oxidation in rod photoreceptors regulates essential fatty acids for retinal visual function

Yan Zeng[1], Chuck T. Chen[2], Mengxu Ge[1], Myriam Boeck[1], Hitomi Yagi[1], Hiroyuki Komatsu[1], Emil Kriukov[3,4], Victoria Hirst[1], Michelle Lee[1], Katherine Neilsen[1], Tommy S. Fong[2], Yan Fu[2], Joshua L. Dunaief[5], James D. Akula[1], Petr Baranov[3,4], Jing Chen[1], Irfan J. Lodhi[6], Richard P. Bazinet[2], Lois E.H. Smith[1], Zhongjie Fu[1,*]

[1]Department of Ophthalmology, Boston Children's Hospital, Harvard Medical School, Boston, MA 02115, USA.
[2]Department of Nutritional Sciences, Temerty Faculty of Medicine, University of Toronto, Toronto, Ontario M5S 1A8, Canada.
[3]Massachusetts Eye and Ear, Boston, MA, 02115, USA.
[4]Department of Ophthalmology, Harvard Medical School, Boston, MA 02115, USA.
[5]F.M. Kirby Center for Molecular Ophthalmology, Scheie Eye Institute, Perelman School of Medicine at the University of Pennsylvania, Philadelphia, PA 19104, USA.
[6]Division of Endocrinology, Metabolism and Lipid Research; Department of Medicine, Washington University, St. Louis, MO 63110, USA.
[*]Corresponding author:
Zhongjie Fu, PhD (email: zhongjie.fu@childrens.harvard.edu), Department of Ophthalmology, Boston Children's Hospital, Harvard Medical School, 3 Blackfan Circle, CLS 18, Boston, MA 02115, USA. Tel: (+1) 617 919 2534.

Abstract

Dyslipidemia contributes to many eye disorders, yet retinal lipid processing remains poorly understood. Deficiency of essential lipid docosahexaenoic acid (DHA) has been reported in many retinal disorders but clinical trials with oral DHA intake had inconsistent findings. In our recent study, we found that despite dietary availability of pre-formed docosahexaenoic acid (DHA), systemic loss of acyl-coenzyme A oxidase 1 (*Acox1*, key in peroxisomal fatty acid oxidation) decreased retinal DHA levels in mice, highlighting a local retinal regulation of DHA homeostasis. To further validate the local retinal cell contribution to DHA control, we used mice with rod photoreceptors-, or retinal pigment epithelium (RPE)-specific loss of *Acox1*, alongside global *Acox1* deficient mice for comparison. At postnatal (P) 30, fatty acid profiling was conducted in isolated retinas and eyecups (RPE, choroid and sclera complex) and retinal visual function was assessed. We found that although there was pre-formed DHA available in the diets, systemic *Acox1* and rod-specific *Acox1* deficiency decreased retinal DHA, without affecting eyecup DHA levels. RPE-*Acox1* deficiency showed no change. Similar to systemic *Acox1* loss, rod or RPE *Acox1* deficiency impaired retinal visual function. These findings highlighted local contribution of peroxisomal ACOX1 to DHA maintenance and neural retinal growth. This advances our knowledge of DHA homeostasis in neural tissue and implicates peroxisomal dysfunction in dyslipidemia-related retinal disorders.

Keywords: peroxisomal fatty acid oxidation; ACOX1; retinal lipid homeostasis; retinal DHA; retinal function

Introduction

Human lipidome changes occurring at around age 44 with additional alternations occur around 60[1]. Dyslipidemia is associated with age-related retinal degeneration and with ocular pathology in peroxisomal disorders. Lipids are essential components of retinal membranes, particularly photoreceptor outer segments, and serve as metabolic substrates for mitochondrial energy production through fatty acid β-oxidation (FAO)[2-4]. Despite increasing recognition of the contribution of FAO to retinal metabolism, its role in maintaining retinal lipid homeostasis and its potential impact on retinal function remains unclear.

FAO occurs in peroxisome and mitochondria. While mitochondria preferentially oxidize long-chain fatty acids (LCFA, 13-21 carbons), peroxisomes primarily oxidize very long-chain fatty acids (VLCFA, ≥22 carbons) to shorter-chain lipids, fueling mitochondrial FAO[5]. Peroxisomes FAO is initiated by acyl-coenzyme A oxidase 1 (ACOX1)-catalyzed dehydrogenation[5]. Mutations in *ACOX1* cause early-onset and progressive neurodegeneration, early retinal dysfunction and pigmentary retinopathy in affected children[6]. *Acox1* deficiency leads to vision loss in mice[7] and flies[8]. In mice, systemic *Acox1* knockout increased liver C22-28 omega-3 (n-3) and omega-6 (n-6) polyunsaturated fatty acids (PUFA) levels, and docosahexaenoic acid (DHA) were unchanged compared to heterozygote controls[9]. In the retina, systemic *Acox1* knockout mice had largely decreased n-3 PUFAs including DHA, with a compensatory increase in n-6 PUFAs compared with wild-type (WT) littermates[7]. These reports suggest that peroxisomal FAO defects can induce tissue-specific effects on PUFA compositions.

Currently our limited understanding of peroxisomal FAO in retinal development, function, and lipid homeostasis is mainly from animal studies. Mice with systemic impairment of peroxisomal function (*Pex1* encoding peroxisomal biogenesis factor 1, or *Mfp2* encoding multifunctional protein 2 deficiency) exhibit reduced electroretinogram (ERG) signals and decreased photoreceptor inner/outer segment thickness during the first 2-3 postnatal weeks[10, 11]. Photoreceptors and bipolar cell-specific knockdown of *Mfp2* in mice impairs rod bipolar cell function at 6 months[12]. RPE-specific loss of *Mfp2* in mice resulted in lysosomal dysfunction and retinal pigment epithelium (RPE) degeneration at 3 weeks[13]. Systemic loss of *Mfp2* reduced retinal DHA levels[14] and RPE DHA-containing phospholipids[13] at 3-4 week-old in mice. In PEX1-p.Gly844Asp (G844D) mouse model with RPE degeneration shown at 3 months, decreased RPE DHA-containing phospholipids were observed early at 1 month old[15]. However, how peroxisomal FAO across distinct retinal cell types contributes to fatty acid profile and visual function remains unclear. To address this, we utilized mutant mice with cell-specific loss of *Acox1* in rod photoreceptors or RPE, along with systemic *Acox1* deficient mice as a reference for comparison.

Methods

Mice

Mice were fed on Prolab IsoPro RMH 3000 standard mouse chow. Mice with systemic knockout of *Acox1* (*Acox1*$^{-/-}$) were obtained from heterozygous breeders[16] (Jackson Laboratory, # 029747, Bar Harbor, ME, USA). We crossed rod photoreceptor-specific *Rho-iCre* mice[17] (Jackson Laboratory, # 015850), or RPE-specific *Best1Cre* mice[18] with *Acox1*$^{flox/flox}$ mice[19] (from Dr. Irfan J. Lodhi, Washington University School of Medicine, under MTA) to generate *Rho-iCre:Acox1*$^{fl/fl}$ and *Best1Cre:Acox1*$^{fl/fl}$ mice. *Rho-iCre,* and *Best1Cre* mice were bred with C57BL/6J (Jackson Laboratory, # 000664) to generate *Cre+* only non-floxed control mice. Mouse genotypes were examined using Transnetyx, Inc (Cordova, TN, USA).

Targeted fatty acid profiling

Eyecups (RPE, choroid and sclera complex) and retina samples from P30 *Acox1*$^{-/-}$ vs. wild-type (WT; *Acox1*$^{+/+}$) mice *(*n=17-18 mice, both retinas or eyecups from the same mouse were pooled as n=1*), or Cre+* vs. littermate *Cre-* mice with cell-specific loss of *Acox1* underwent total fatty acid profiling (n=3-6 mice). As previously described[7], total lipids were extracted from weighed eyecups and retinas with serial addition of 0.88% potassium chloride, methanol, and chloroform (0.88:1:2 v/v). Heptadecanoic acid (17:0) was added to the total lipid extract as an internal standard. Total lipids were methylated with boron trifluoride in methanol at 100^{o}C for an hour. Fatty acid methyl esters (FAMEs) were separated with a gas chromatograph equipped with flame ionization detector (Varian-430 GC, Bruker) on a DB-FFAP (30 m x 0.25 mm i.d. x 0.25 µm film thickness) column. The run methods were set at initial oven temperature of 50^{o}C (1 min), then a ramp to 130^{o}C (30^{o}C/min), 175^{o}C (10^{o}C/min), 230^{o}C (5^{o}C/min, held 9.5 min), and 240^{o}C (50^{o}C/min, 11.13 min). Concentration of FAs (nmol/g) were quantified by peak comparison to C17:0. Fatty acid profiles were provided in **Supplemental Table 1**.

Western blot

RPE from P30 *Cre+* vs. littermate *Cre- Best1Cre:Acox1*$^{fl/fl}$ mice were isolated following a previously published protocol[20]. Briefly, the RPE/choroid/sclera complex was cut radially at four locations using scissors to flatten the tissue and then incubated in 100 µL of RIPA lysis buffer (89900, Thermo Fisher Scientific, Waltham, MA, USA) supplemented with protease inhibitors (1:1000; 87785, Thermo Fisher Scientific) for 20 min on ice with gentle shaking. Following incubation, the choroid/sclera complex was gently removed, leaving the RPE cells in the lysis buffer. The RPE were then incubated for an additional 15 min on ice. Samples were centrifuged at >12,000 × *g* for 15 min at 4°C, and the supernatant containing the total protein lysate was collected for protein concentration measurement and subsequent Western blot analysis.

Retinas from P30 *Cre+* vs. littermate *Cre- Rho-iCre:Acox1*$^{fl/fl}$ mice were pooled, lysed in 80 µL RIPA buffer (89900, Thermo Fisher Scientific) supplemented with protease inhibitors (1:1000; 87785, Thermo Fisher Scientific), and sonicated on ice. Protein concentrations were determined, and 20 µg of total protein lysates were separated on NuPAGE™ 4–12% Bis-Tris gels (NP0322BOX, Thermo Fisher Scientific) and transferred

to 0.2 µm PVDF membranes (88520, Thermo Fisher Scientific). Membranes were blocked with 5% nonfat milk and incubated with anti-ACOX1 antibody (1:1000; AB184032, Abcam, Cambridge, UK), anti-β-ACTIN (1:5000; A1978, Sigma-Aldrich, St. Louis, MO, USA) diluted in 5% bovine serum albumin (BSA) at 4°C overnight. Membranes were incubated with the corresponding horseradish peroxidase-conjugated secondary antibodies (1:10,000) at room temperature, and signals were detected using SuperSignal™ West Pico PLUS Chemiluminescent Substrate (34577, Thermo Fisher Scientific) or SuperSignal™ West Femto Maximum Sensitivity Substrate (34096, Thermo Fisher Scientific), followed by imaging (Azure 600 Imaging System, Dublin, CA, USA). β-ACTIN served as internal control. Both retinas or RPE from the same mouse were pooled as n=1, n=4 mice per group.

ERG

ERG was performed as we previously described[7]. For all strains except *Rho-iCre:Acox1*$^{fl/lf}$ mice, rod ERGs were recorded using an Espion *e*^{2} (Diagnosys LLC, Lowell, MA, USA) in dark-adapted, mydriatic (Cyclomydril; Alcon, Fort Worth, TX, USA), anesthetized (ketamine/xylazine) mice. Stimuli consisted of "green" light emitting diode flashes of increasing intensity (doubling from ~0.00025 to ~2.05 cd·s/m^2), followed by "white" xenon-arc flashes ranging from ~8.2 to ~1,050 cd·s/m^2 presented in an integrating sphere (Colordome, Diagnosys LLC). For *Rho-iCre:Acox1*$^{fl/fl}$ mice, flash ERGs were obtained using a Celeris High Throughput Testing System (Diagnosys LLC). Stimuli consisted of "red" and "green" light-emitting diode flashes of doubling intensity from ~0.00125 to ~65.536 cd·s/m^2. Average ERG plots at selected intensities were shown as indicated in the figure legend.

The *a*-waves representing saturating photo responses were estimated by fitting the free parameters in a model of the biochemical processes involved in the activation of phototransduction to the electroretinographic *a*-waves[21, 22]. The saturating amplitude and sensitivity of second-order neurons, principally bipolar cells[23], was measured by subtracting the mathematical model of the photoreceptor response from the intact ERG waveform[24] and fitting the Naka-Rushton equation[25] to the response vs. intensity relationship of the resulting waveform. Representative ERG plots were generated using average signals from the eyes in each group at 0.001, 0.064, 2.048, 8.192, 16.384, 32.768, 65.536 cd·s/m^2. All ERG data were presented as the log change from control (*Cre+:Acox1*$^{fl/fl}$ vs. *Cre-:Acox1*$^{fl/fl}$, or *Cre+* only mice respectively) (ΔLogControl) at P30.

Gene expression of retinal Acox1 from single-cell analysis

Dotplot of *Acox1,* rod cell marker *Rho,* Müller glia/astrocytes marker *Glul* in mouse retinas was examined using the following online single-cell dataset: "C57B6 wild-type P14 retina by drop-seq". (https://singlecell.broadinstitute.org/single_cell/study/SCP301)[26] at Single Cell Portal, Broad Institute. *Acox1, Rho, Pde6b, Rlbp1* and *Glul* were entered under "Explore", dotplot of gene expression for different cell types was displayed. To further assess *ACOX1* expression in the developing human retina, we re-loaded the publicly available human fetal retina atlas that we previously assembled and

described[27]. The dataset was imported into Seurat v4, and cell-class–specific gene markers were visualized across the relevant populations using the DotPlot function.

Statistics

All data are presented as mean ± SEM. For targeted fatty acid profiling, Welch's *t*-tests with no assumption of equal variance were used. For analysis of ERG and western blot, data normality (quantile-quantile plot) and variance (F-test) were evaluated first, followed by either parametric tests (unpaired t-test or Welch's t-test) or the non-parametric Mann-Whitney U test. (Prism v10.0; GraphPad Software, Inc.). Statistical significance was set at $p < 0.05$.

Results

Acox1 was locally expressed in retinas

ACOX1 was previously detected in RPE and total retinal protein lysates[7, 28]. To further examine the local cell types expressing *Acox1*, we utilized a public single-cell dataset of "C57B6 wild-type P14 retina by drop-seq"[26] at Single Cell Portal, Broad Institute. *Acox1* was expressed across most retinal cells (rods, cones, bipolar, horizontal, amacrine, retinal ganglion cells, and Müller glia/astrocytes) (**Supplemental Fig. 1A**). We further confirmed expression of *ACOX1* in human fetal retina using human fetal retina atlas, with the timepoints spanning week 9 to week 27[27] (**Supplemental Fig. 1B**). These findings suggested that there was local expression of ACOX1 in developing retinas.

Rod peroxisomal FAO controlled retinal DHA levels

We recently reported that systemic loss of *Acox1* in mice reduced most retinal n-3 FAs, with increased n-6 FAs as compensatory responses at P30[7]. Here we included the analysis of both retinal and eyecup (RPE, choroid and sclera complex) FA profiles from mice with systemic loss of *Acox1*(*Acox1*$^{-/-}$) vs. littermate WT (*Acox1*$^{+/+}$) controls. In mice with systemic loss of *Acox1*(*Acox1*$^{-/-}$) vs. littermate WT (*Acox1*$^{+/+}$) controls, there was a decrease in n-3 FAs in the *Acox1*$^{-/-}$ retinas, while n-3 FAs were mostly stable in eyecups (**Fig. 1A, B**). Despite dietary presence of pre-formed eicosapentaenoic acid (EPA), DHA and α-linolenic acid (ALA, 18:3n-3, the precursor of EPA and DHA), retinal DHA (C22:6n-3) was significantly reduced with systemic *Acox1* loss (**Fig. 1A**). DHA level in eyecups remained unchanged (**Fig. 1B**), suggesting that retinal DHA levels might be regulated independently from RPE transport and circulating DHA pools.

To further clarify the local peroxisomal FAO's role in lipid balance, we profiled total FAs in retinas and eyecups from mice with rod-, or RPE-specific loss of *Acox1* at P30. In *Rho-iCre* strain, iCre-mediated genomic DNA excision approaches adult levels at P30 and Cre protein expression is near the plateau measured at 2 months[17]. Decreased retinal ACOX1 levels in P30 *Cre+* vs. *Cre- Rho-iCre:Acox1*$^{fl/fl}$ mice were confirmed with western blot (**Fig. 2A**). With same diet provided, there was a profound decrease in essential DHA

and EPA (C20:5n-3) in retinas from mice with rod *Acox1* deficiency (**Fig. 2B**), while DHA and EPA levels were unchanged in eyecups (**Fig. 2C**).

In *Best1Cre* line, Cre becomes detectable in the RPE by P10, reaches stable adult levels by P28, and remains confined to RPE nuclei in a mosaic pattern covering roughly 50-70% of cells at 1 month[18]. ACOX1 protein levels were significantly decreased in RPE isolated from P30 *Cre+* vs. *Cre- Best1Cre:Acox1$^{fl/fl}$* mice (**Fig. 3A**). In mice with RPE *Acox1* deficiency, no significant changes were found in either retinal or eyecup FAs (**Fig. 3B, C**).

In the *de novo* DHA synthesis, peroxisomal β-oxidation converts C24 intermediates (C24:6n-3) to DHA (**Supplemental Fig. 2A**). DHA can be retroconverted back to EPA[29], however, this capacity might be very limited in mammals[30, 31]. C24/C22 fatty acid ratio is often used as a marker for peroxisomal function[32] and retinal C24:0/C22:0 ratio was increased with systemic *Acox1* loss[7]. Further analysis also showed comparable C24:6n-3/C22:6n-3 ratio in retinas (**Supplemental Fig. 2B**). There was significantly increased C24:6n-3/C22:6n-3 ratio (p = 0.0002) and comparable C24:0/C22:0 ratio in the eyecups with systemic *Acox1* loss (**Supplemental Fig. 2C**). These findings suggested that retinas and RPE seemed to have different substrate preferences for oxidating VLCFA. However, systemic availability can influence ocular fatty acid levels and impact the C24/C22 ratio. We therefore assessed whether cell-type-specific *Acox1* deletion altered C24/C22 ratios. Neither rod- nor RPE-specific *Acox1* deficiency significantly affected C24:6n-3/C22:6n-3 or C24:0/C22:0 ratios in retinas or eyecups, respectively (**Supplemental Fig. 2D, E**). These results suggested that neighboring cell types, systemic clearance, or intrinsic cellular compensatory pathways preserved local lipid homeostasis when peroxisomal FAO was selectively impaired.

Local loss of Acox1 caused visual defects in the neural retina

To further investigate the local contribution of peroxisomal FAO to neural retinal development, visual function was evaluated at P30 with ERG. Amplitude, which reflects total number of functioning cells, and sensitivity, which reflects efficiency of retinal responses to light intensity, were examined for *a*-wave (photoreceptors) and *b*-wave (bipolar cells). Since Cre recombinase expression may influence retinal health[33], we first confirmed that Cre expression in RPE not in rods increased amplitude *a*- and *b*- wave (**Supplemental Fig. 3**). We therefore compared ERG signals of *Cre+:Acox1$^{fl/fl}$* mice with 1) littermate *Cre-:Acox$^{fl/fl}$* mice, and 2) *Cre+* only control mice.

P30 *Cre+* vs*. Cre- Rho-iCre:Acox1$^{fl/fl}$* mice had decreased amplitudes of *a*-wave (rod photoreceptor), a trend of decrease in amplitude of *b*-wave (rod bipolar cells), and a trend of decrease in sensitivity of *a*-wave and *b*-wave (**Fig. 4A, B**). When compared to *Cre+ Rho-iCre* only non-floxed control mice, *Cre+ Rho-iCre:Acox1$^{fl/fl}$* mice had decreased amplitudes and increased sensitivity of *a*-wave and *b*-wave (**Fig. 4C**). The increased sensitivity might compensate for the reduced amplitude[34]. These findings suggested that peroxisomal FAO in rod photoreceptors contributed to rod pathway signaling.

We also found decreased amplitudes of *a*-wave and *b*-wave in *Cre+* vs. *Cre-Best1Cre:Acox1*$^{fl/fl}$ mice (**Fig. 5A, B**). When compared with *Cre+ Best1Cre* only non-floxed control mice, a trend of decrease in amplitudes of *a*-wave and a significant decrease in amplitudes of *b*-wave were found (**Fig. 5C**). These findings suggested that peroxisomal FAO in RPE supported rod photoreceptors and the downstream bipolar cell signaling.

Taken together, our findings suggested that there was a local regulation of retinal DHA homeostasis and peroxisomal ACOX1-mediated pathway in local rods or RPE cells contributed to neural retinal function.

Discussion and conclusion

Deficiency in DHA is found in many retinal disorders[35]. However, the outcomes of DHA supplementation on retinal diseases are inconsistent[35]. Dietary change can significantly modulate retinal DHA levels[36-41], but retinal DHA levels seemed resistant to dietary excess[42, 43]. We recently showed that increasing dietary DHA supplementation (3% vs. 1% DHA of total lipids) increased plasma and eyecups (RPE, choroid and sclera complex) DHA but did not further increase retinal DHA content in neonatal mice[42], suggesting tight regulation of retinal DHA. This ceiling effect is further evidenced by studies using deuterated (D)-DHA; when introduced to the diet, the labeled DHA merely replaced existing stores within the retina rather than increasing the overall pool size[43]. Yet, the underlying mechanism regulating retinal DHA remains unclear.

In this study, we found that ACOX1 in rod photoreceptors contributed to the maintenance of DHA and EPA in the retinas. RPE possibly maintained its EPA and DHA level from circulating pre-formed dietary EPA and DHA. Despite the presence of DHA and its precursor ALA in the diet, rod *Acox1* deficiency decreased DHA in mouse retina not in eyecup, suggesting that retinal DHA homeostasis was strictly controlled, possibly mediated by peroxisomal ACOX1 in rod photoreceptors. In future investigations to gain further mechanistic insight into the regulatory pathways, we will assess the impact of rod *Acox1* deficiency on DHA uptake and retention proteins such as major facilitator superfamily domain containing 2a[44, 45], adiponectin receptor protein 1 (ADIPOR1)[46, 47], acyl-CoA synthetase 6 (ACSL6) and lysophosphatidic acid acyltransferase 3 (LPAAT3)[48, 49]. The final step of *de novo* DHA synthesis is the conversion of n-3 VLCPUFA (C24:6n-3) into DHA by peroxisomal β-oxidation[50]. Neural retina possesses a very limited capacity for synthesizing DHA from its precursor ALA, we therefore speculate that these C24 intermediates come from systemic circulation[51] or RPE through the recycling of shed photoreceptor outer segment lipids[52]. We observed a significant decrease in DHA and a trend of increased C24:6n-3/C22:6n-3 ratio ($p = 0.054$) in retinas with rod *Acox1* deficiency, suggesting potentially compromised peroxisomal β-oxidation of C24:6n-3 due to the loss of *Acox1* in rods. Circulating DHA might replenish DHA pool in eyecups with RPE *Acox1* deficiency, while this buffering effect was masked in retinas with rod *Acox1* deficiency. Future studies targeting at rods' contribution to n3 VLCPUFA processing are needed to fill our current knowledge gap of DHA regulation in the retina.

Interestingly, C24:0/C22:0 ratio was unchanged with neither rod nor RPE loss of *Acox1*. We have recently reported increased mitochondrial FAO proteins in retinas with global loss of *Acox1*[7]. Mitochondria possess some capacity to oxidize saturated and monounsaturated VLCFAs (C24:0, C24:1)[53], we speculate that mitochondrial compensation might maintain C24:0/C22:0 ratio while ACOX1 protein was deficient in rod or RPE cells. Systemic loss of *Acox1* decreased retinal glycolytic proteins, mitochondrial substrate pyruvate, and mitochondrial number in photoreceptor inner segments[7]. Supplementation of pyruvate delayed the progression of retinal visual dysfunction during development[7]. These findings showed that loss of *Acox1* caused severe energy crisis and subsequent visual abnormalities which triggered mitochondrial FAO compensation to sustain energy production and preserve visual function. However, increased mitochondrial FAO might increase oxidative stress[54]. The cell functional outcome of compensatory mitochondrial FAO in response to compromised peroxisomal FAO needs to be further evaluated. It is also possible that other neighboring retinal cells types handle saturated VLCFA turnover while rod photoreceptors preferred to shorten C24:6n3, as indicated by local gene expression of *Acox1* in other retinal cell types.

The functional integrity of rod photoreceptor cells depends on a specialized lipid environment within photoreceptor outer segments[55]. Rod lipid composition transitions from a saturated FA to an unsaturated FA environment during postnatal development in mice, with DHA increasing steadily across major phospholipid classes[56]. Retina and photoreceptor outer segment is highly enriched in DHA[57]. DHA deficiency causes increased membrane rigidity, disordered disc morphology, compensatory changes in phospholipid composition and impaired retinal visual function[45, 48]. Long-term dietary DHA deficiency in monkeys led to age-dependent loss in rod sensitivity and delayed rod recovery for bright saturating flashes while cone phototransduction was not altered[58]. Maintaining lipid homeostasis is therefore critical for neural retinal development and visual function. Photoreceptors have high energy demand and depend on their supporting cells like RPE and Müller glia for coordinated glucose and lipid support[59, 60]. Correspondingly, we here found consistent decreases in amplitudes of rod *a*-wave in both strains, indicating decreased total number of functional rod photoreceptors.

Despite retinal visual dysfunction we found with cell-specific loss of *Acox1* in RPE, there were no obvious changes in retinal DHA levels. We could not exclude the possibility that contribution from RPE to retinal DHA levels was masked by rods which account for about 66% of total retinal cells[26]. The underlying mechanisms behind RPE peroxisomal FAO contribution to photoreceptor function need further exploration. Unlike retina, eyecup (RPE, choroid and sclera complex) fatty acid profiles were unchanged in both strains, which were possibly maintained from circulating pre-formed dietary DHA, suggesting distinct mechanisms to preserve DHA in RPE. However, our findings were also limited because fatty acid analysis of the RPE/choroid/sclera complex could mask localized changes within the RPE alone. Further improvement in technique by utilizing isolated RPE fatty acid profiling will be necessary to confirm our results. Finally, although the C24:0/C22:0 ratio is widely used as a marker for peroxisomal FAO, mitochondria also

possessed the capacity to oxidize these fatty acids[53]. Future analysis including longer-chain FAs, like C26:0 and above, could further complement the current findings.

Taken together, our current work found that loss of *Acox1* in rod photoreceptors reduced retinal DHA, highlighting the role of rod-specific peroxisomal FAO in regulating retinal DHA despite the availability of dietary DHA. Modulating peroxisomal FAO could be a potential approach to treat dyslipidemia-related retinal disorders.

List of abbreviations

Acox1: acyl-coenzyme A oxidase 1
ALA: α-linolenic acid
DHA: docosahexaenoic acid
EPA: eicosapentaenoic acid
ERG: electroretinogram
FAO: fatty acid β-oxidation
Mfp2: multifunctional protein 2 deficiency
RPE: retinal pigment epithelium
Pex1: peroxisomal biogenesis factor 1
PUFA: polyunsaturated fatty acid
VLCFA: very long-chain fatty acid
WT: wild-type

Declarations

Ethics approval and consent to participate

All mouse experiments followed Association for Research in Vision and Ophthalmology Statement for Use of Animals in Ophthalmic Vision and Research and the National Institutes of Health Guide for the Care and Use of Laboratory Animals (NIH Publications No. 8523, revised 2011) and was approved by Boston Children's Hospital's Institutional Animal Care and Use Committee (protocols #00002500 and #00002586).

Consent for publication

Not applicable.

Availability of data and materials

The fatty acid profiling data generated in this study are provided as supplementary information. Additional datasets used and/or analyzed during the current study are available from the corresponding author on reasonable request.

Competing interests

JC serves as a consultant to EyePoint Pharmaceuticals. The authors have no other competing interests to declare.

Funding

The work was supported by NIH/NEI R01 grants (EY017017, EY032492), Boston Children's Hospital (OFD/BTREC/CTREC Faculty Career Development Grant 97906, Ophthalmology Foundation 85010), Mass Lions Eye Foundation Inc., 78158, Knight's Templar Eye Research Endowment Fund 87821 (ZF); NIH/NEI R01 grants (EY024963, EY028100, and EY031765), BrightFocus Foundation, Boston Children's Hospital Ophthalmology Foundation (JC); NIH/NEI EY017017, BCH IDDRC (1U54HD090255), Massachusetts Lions Eye Foundation 79246 (LEHS).

The "Public Access Policy" of the National Institutes of Health mandates that Author Accepted Manuscripts arising from NIH-funded research must be made available in PubMed Central immediately upon publication. By accepting this manuscript, which arose from NIH-funded research, the Journal agrees that it will not impose a fee for the author's compliance with the NIH Policy, notwithstanding any agreement or policy of the Journal to the contrary.

Authors' contributions

Conceptualization, ZF; data curation, formal analysis, YZ, CTC, MG, MB, HY, HK, EK, VH, ML, KN, TF, YF; writing – original draft, ZF, YZ, MG; expert advice and reviewing and editing the manuscript, CTC, MB, HY, JLD, JDA, PB, JC, IJL, RB, LEHS; funding acquisition, ZF, LEHS, JC.

ZF had full access to all the data in the study. All authors have read the final version of the manuscript.

References

1. Shen X, Wang C, Zhou X, Zhou W, Hornburg D, Wu S, Snyder MP: **Nonlinear dynamics of multi-omics profiles during human aging.** *Nat Aging* 2024.
2. Joyal JS, Sun Y, Gantner ML, Shao Z, Evans LP, Saba N, Fredrick T, Burnim S, Kim JS, Patel G, et al: **Retinal lipid and glucose metabolism dictates angiogenesis through the lipid sensor Ffar1.** *Nat Med* 2016, **22:**439–445.
3. Agbaga MP, Merriman DK, Brush RS, Lydic TA, Conley SM, Naash MI, Jackson S, Woods AS, Reid GE, Busik JV, Anderson RE: **Differential composition of DHA and very-long-chain PUFAs in rod and cone photoreceptors.** *J Lipid Res* 2018, **59:**1586–1596.
4. Fu Z, Kern TS, Hellstrom A, Smith LEH: **Fatty acid oxidation and photoreceptor metabolic needs.** *J Lipid Res* 2021, **62:**100035.
5. Chen CT, Shao Z, Fu Z: **Dysfunctional peroxisomal lipid metabolisms and their ocular manifestations.** *Front Cell Dev Biol* 2022, **10:**982564.
6. Poll-The BT, Saudubray JM, Ogier HA, Odievre M, Scotto JM, Monnens L, Govaerts LC, Roels F, Cornelis A, Schutgens RB, et al.: **Infantile Refsum disease: an inherited peroxisomal disorder. Comparison with Zellweger syndrome and neonatal adrenoleukodystrophy.** *Eur J Pediatr* 1987, **146:**477–483.
7. Boeck M, Yagi H, Chen CT, Zeng Y, Lee D, Nian S, Kasai T, Lee J, Hirst V, Wang C, et al: **Nutrient supplementation mitigates retinal dysfunction in Acox1 knockout mice with impaired peroxisomal fatty acid oxidation.** *J Adv Res* 2025.
8. Chung HL, Wangler MF, Marcogliese PC, Jo J, Ravenscroft TA, Zuo Z, Duraine L, Sadeghzadeh S, Li-Kroeger D, Schmidt RE, et al: **Loss- or Gain-of-Function Mutations in ACOX1 Cause Axonal Loss via Different Mechanisms.** *Neuron* 2020, **106:**589–606 e586.
9. Infante JP, Tschanz CL, Shaw N, Michaud AL, Lawrence P, Brenna JT: **Straight-chain acyl-CoA oxidase knockout mouse accumulates extremely long chain fatty acids from alpha-linolenic acid: evidence for runaway carousel-type enzyme kinetics in peroxisomal beta-oxidation diseases.** *Mol Genet Metab* 2002, **75:**108–119.
10. Argyriou C, Polosa A, Cecyre B, Hsieh M, Di Pietro E, Cui W, Bouchard JF, Lachapelle P, Braverman N: **A longitudinal study of retinopathy in the PEX1-Gly844Asp mouse model for mild Zellweger Spectrum Disorder.** *Exp Eye Res* 2019, **186:**107713.
11. Das Y, Swinkels D, Kocherlakota S, Vinckier S, Vaz FM, Wever E, van Kampen AHC, Jun B, Do KV, Moons L, et al: **Peroxisomal Multifunctional Protein 2 Deficiency Perturbs Lipid Homeostasis in the Retina and Causes Visual Dysfunction in Mice.** *Front Cell Dev Biol* 2021, **9:**632930.
12. Swinkels D, Das Y, Kocherlakota S, Vinckier S, Wever E, van Kampen AHC, Vaz FM, Baes M: **Cell Type-Selective Loss of Peroxisomal beta-Oxidation Impairs Bipolar Cell but Not Photoreceptor Survival in the Retina.** *Cells* 2022, **11**.
13. Kocherlakota S, Das Y, Swinkels D, Vanmunster M, Callens M, Vinckier S, Vaz FM, Sinha D, Van Veldhoven PP, Fransen M, Baes M: **The murine retinal pigment epithelium requires peroxisomal beta-oxidation to maintain lysosomal function and prevent dedifferentiation.** *Proc Natl Acad Sci U S A* 2023, **120:**e2301733120.
14. Swinkels D, Kocherlakota S, Das Y, Dane AD, Wever EJM, Vaz FM, Bazan NG, Van Veldhoven PP, Baes M: **DHA Shortage Causes the Early Degeneration of Photoreceptors and RPE in Mice With Peroxisomal beta-Oxidation Deficiency.** *Invest Ophthalmol Vis Sci* 2023, **64:**10.
15. Omri S, Argyriou C, Pryce RS, Di Pietro E, Chaurand P, Braverman N: **Spatial characterization of RPE structure and lipids in the PEX1-p.Gly844Asp mouse model for Zellweger spectrum disorder.** *J Lipid Res* 2025, **66:**100771.

16. Fan CY, Pan J, Chu R, Lee D, Kluckman KD, Usuda N, Singh I, Yeldandi AV, Rao MS, Maeda N, Reddy JK: **Hepatocellular and hepatic peroxisomal alterations in mice with a disrupted peroxisomal fatty acyl-coenzyme A oxidase gene.** *J Biol Chem* 1996, **271:**24698–24710.
17. Li S, Chen D, Sauve Y, McCandless J, Chen YJ, Chen CK: **Rhodopsin-iCre transgenic mouse line for Cre-mediated rod-specific gene targeting.** *Genesis* 2005, **41:**73–80.
18. Iacovelli J, Zhao C, Wolkow N, Veldman P, Gollomp K, Ojha P, Lukinova N, King A, Feiner L, Esumi N, et al: **Generation of Cre transgenic mice with postnatal RPE-specific ocular expression.** *Invest Ophthalmol Vis Sci* 2011, **52:**1378–1383.
19. Park H, He A, Tan M, Johnson JM, Dean JM, Pietka TA, Chen Y, Zhang X, Hsu FF, Razani B, et al: **Peroxisome-derived lipids regulate adipose thermogenesis by mediating cold-induced mitochondrial fission.** *J Clin Invest* 2019, **129:**694–711.
20. Huang S, Liu CH, Wang Z, Fu Z, Britton WR, Blomfield AK, Kamenecka TM, Dunaief JL, Solt LA, Chen J: **REV-ERBalpha regulates age-related and oxidative stress-induced degeneration in retinal pigment epithelium via NRF2.** *Redox Biol* 2022, **51:**102261.
21. Lamb TD, Pugh EN, Jr.: **A quantitative account of the activation steps involved in phototransduction in amphibian photoreceptors.** *J Physiol* 1992, **449:**719–758.
22. Pugh EN, Jr., Lamb TD: **Amplification and kinetics of the activation steps in phototransduction.** *Biochim Biophys Acta* 1993, **1141:**111–149.
23. Wurziger K, Lichtenberger T, Hanitzsch R: **On-bipolar cells and depolarising third-order neurons as the origin of the ERG-b-wave in the RCS rat.** *Vision Res* 2001, **41:**1091–1101.
24. Robson JG, Frishman LJ: **Response linearity and kinetics of the cat retina: the bipolar cell component of the dark-adapted electroretinogram.** *Vis Neurosci* 1995, **12:**837–850.
25. Fulton AB, Rushton WA: **The human rod ERG: correlation with psychophysical responses in light and dark adaptation.** *Vision Res* 1978, **18:**793–800.
26. Macosko EZ, Basu A, Satija R, Nemesh J, Shekhar K, Goldman M, Tirosh I, Bialas AR, Kamitaki N, Martersteck EM, et al: **Highly Parallel Genome-wide Expression Profiling of Individual Cells Using Nanoliter Droplets.** *Cell* 2015, **161:**1202–1214.
27. Kriukov E, Soucy JR, Labrecque E, Baranov P: **Unraveling the developmental heterogeneity of human retinal ganglion cells within the developing retina to study to the continuity of maturation.** *Dev Biol* 2025, **528:**91–104.
28. Das Y, Roose N, De Groef L, Fransen M, Moons L, Van Veldhoven PP, Baes M: **Differential distribution of peroxisomal proteins points to specific roles of peroxisomes in the murine retina.** *Mol Cell Biochem* 2019, **456:**53–62.
29. Park HG, Lawrence P, Engel MG, Kothapalli K, Brenna JT: **Metabolic fate of docosahexaenoic acid (DHA; 22:6n-3) in human cells: direct retroconversion of DHA to eicosapentaenoic acid (20:5n-3) dominates over elongation to tetracosahexaenoic acid (24:6n-3).** *FEBS Lett* 2016, **590:**3188–3194.
30. Metherel AH, Irfan M, Klingel SL, Mutch DM, Bazinet RP: **Compound-specific isotope analysis reveals no retroconversion of DHA to EPA but substantial conversion of EPA to DHA following supplementation: a randomized control trial.** *Am J Clin Nutr* 2019, **110:**823–831.
31. Metherel AH, Chouinard-Watkins R, Trepanier MO, Lacombe RJS, Bazinet RP: **Retroconversion is a minor contributor to increases in eicosapentaenoic acid following docosahexaenoic acid feeding as determined by compound specific isotope analysis in rat liver.** *Nutr Metab (Lond)* 2017, **14:**75.
32. Morales-Romero B, Gonzalez de Aledo-Castillo JM, Fernandez Sierra C, Martinez Carreira C, Zaragoza Bonet C, Fernandez Bonifacio R, Caro Miro MA, Argudo-Ramirez A, Lopez Galera RM, Garcia-Villoria J: **Plasma C24:0- and C26:0-lysophosphatidylcholines are reliable**

biomarkers for the diagnosis of peroxisomal beta-oxidation disorders. *J Lipid Res* 2024, **65:**100516.

33. He L, Marioutina M, Dunaief JL, Marneros AG: **Age- and gene-dosage-dependent cre-induced abnormalities in the retinal pigment epithelium.** *Am J Pathol* 2014, **184:**1660–1667.
34. Leinonen HO, Bull E, Fu Z: **Neural and Muller glial adaptation of the retina to photoreceptor degeneration.** *Neural Regen Res* 2023, **18:**701–707.
35. Gong Y, Fu Z, Liegl R, Chen J, Hellstrom A, Smith LE: **omega-3 and omega-6 long-chain PUFAs and their enzymatic metabolites in neovascular eye diseases.** *Am J Clin Nutr* 2017, **106:**16–26.
36. Schnebelen C, Gregoire S, Pasquis B, Joffre C, Creuzot-Garcher CP, Bron AM, Bretillon L, Acar N: **Dietary n-3 and n-6 PUFA enhance DHA incorporation in retinal phospholipids without affecting PGE(1) and PGE (2) levels.** *Lipids* 2009, **44:**465–470.
37. Delton-Vandenbroucke I, Maude MB, Chen H, Aguirre GD, Acland GM, Anderson RE: **Effect of diet on the fatty acid and molecular species composition of dog retina phospholipids.** *Lipids* 1998, **33:**1187–1193.
38. Carrie I, Smirnova M, Clement M, De JD, Frances H, Bourre JM: **Docosahexaenoic acid-rich phospholipid supplementation: effect on behavior, learning ability, and retinal function in control and n-3 polyunsaturated fatty acid deficient old mice.** *Nutr Neurosci* 2002, **5:**43–52.
39. Wang JY, Saito M: **Dietary supplementation of N-3 fatty acids and hydroperoxide levels in rat retinas.** *Free Radic Res* 2001, **35:**367–375.
40. Weisinger HS, Vingrys AJ, Bui BV, Sinclair AJ: **Effects of dietary n-3 fatty acid deficiency and repletion in the guinea pig retina.** *Invest Ophthalmol Vis Sci* 1999, **40:**327–338.
41. Connor KM, SanGiovanni JP, Lofqvist C, Aderman CM, Chen J, Higuchi A, Hong S, Pravda EA, Majchrzak S, Carper D, et al: **Increased dietary intake of omega-3-polyunsaturated fatty acids reduces pathological retinal angiogenesis.** *Nat Med* 2007, **13:**868–873.
42. Boeck M, Yagi H, Lundgren P, Pivodic A, Nilsson AK, Zeng Y, Chen CT, Kasai T, Lee D, Nian S, et al: **Combined dietary omega-3 and omega-6 fatty acids protect against hyperglycemia-associated retinopathy in neonatal mice.** *Pharmacol Res* 2025, **219:**107877.
43. James G, Bohannan W, Adewunmi E, Schmidt K, Park HG, Shchepinov MS, Agbaga MP, Brenna JT: **Pharmacokinetics and metabolism in mouse retina of bis-allylic deuterated docosahexaenoic acid (D-DHA), a new dry AMD drug candidate.** *Exp Eye Res* 2022, **222:**109193.
44. Wong BH, Chan JP, Cazenave-Gassiot A, Poh RW, Foo JC, Galam DL, Ghosh S, Nguyen LN, Barathi VA, Yeo SW, et al: **Mfsd2a Is a Transporter for the Essential omega-3 Fatty Acid Docosahexaenoic Acid (DHA) in Eye and Is Important for Photoreceptor Cell Development.** *J Biol Chem* 2016, **291:**10501–10514.
45. Lobanova ES, Schuhmann K, Finkelstein S, Lewis TR, Cady MA, Hao Y, Keuthan C, Ash JD, Burns ME, Shevchenko A, Arshavsky VY: **Disrupted Blood-Retina Lysophosphatidylcholine Transport Impairs Photoreceptor Health But Not Visual Signal Transduction.** *J Neurosci* 2019, **39:**9689–9701.
46. Rice DS, Calandria JM, Gordon WC, Jun B, Zhou Y, Gelfman CM, Li S, Jin M, Knott EJ, Chang B, et al: **Adiponectin receptor 1 conserves docosahexaenoic acid and promotes photoreceptor cell survival.** *Nat Commun* 2015, **6:**6228.
47. Osada H, Toda E, Homma K, Guzman NA, Nagai N, Ogawa M, Negishi K, Arita M, Tsubota K, Ozawa Y: **ADIPOR1 deficiency-induced suppression of retinal ELOVL2 and**

docosahexaenoic acid levels during photoreceptor degeneration and visual loss. *Cell Death Dis* 2021, **12:**458.

48. Shindou H, Koso H, Sasaki J, Nakanishi H, Sagara H, Nakagawa KM, Takahashi Y, Hishikawa D, Iizuka-Hishikawa Y, Tokumasu F, et al: **Docosahexaenoic acid preserves visual function by maintaining correct disc morphology in retinal photoreceptor cells.** *J Biol Chem* 2017, **292:**12054–12064.
49. Kuroha S, Katada Y, Isobe Y, Uchino H, Shishikura K, Nirasawa T, Tsubota K, Negishi K, Kurihara T, Arita M: **Long chain acyl-CoA synthetase 6 facilitates the local distribution of di-docosahexaenoic acid- and ultra-long-chain-PUFA-containing phospholipids in the retina to support normal visual function in mice.** *FASEB J* 2023, **37:**e23151.
50. Wang N, Anderson RE: **Synthesis of docosahexaenoic acid by retina and retinal pigment epithelium.** *Biochemistry* 1993, **32:**13703–13709.
51. Bazan NG, Rodriguez de Turco EB, Gordon WC: **Pathways for the uptake and conservation of docosahexaenoic acid in photoreceptors and synapses: biochemical and autoradiographic studies.** *Can J Physiol Pharmacol* 1993, **71:**690–698.
52. Bazan NG, Calandria JM, Serhan CN: **Rescue and repair during photoreceptor cell renewal mediated by docosahexaenoic acid-derived neuroprotectin D1.** *J Lipid Res* 2010, **51:**2018–2031.
53. Sandhir R, Khan M, Chahal A, Singh I: **Localization of nervonic acid beta-oxidation in human and rodent peroxisomes: impaired oxidation in Zellweger syndrome and X-linked adrenoleukodystrophy.** *J Lipid Res* 1998, **39:**2161–2171.
54. Turrens JF: **Mitochondrial formation of reactive oxygen species.** *J Physiol* 2003, **552:**335–344.
55. Fliesler SJ, Anderson RE: **Chemistry and metabolism of lipids in the vertebrate retina.** *Prog Lipid Res* 1983, **22:**79–131.
56. Scott BL, Racz E, Lolley RN, Bazan NG: **Developing rod photoreceptors from normal and mutant Rd mouse retinas: altered fatty acid composition early in development of the mutant.** *J Neurosci Res* 1988, **20:**202–211.
57. Stinson AM, Wiegand RD, Anderson RE: **Fatty acid and molecular species compositions of phospholipids and diacylglycerols from rat retinal membranes.** *Exp Eye Res* 1991, **52:**213–218.
58. Jeffrey BG, Neuringer M: **Age-related decline in rod phototransduction sensitivity in rhesus monkeys fed an n-3 fatty acid-deficient diet.** *Invest Ophthalmol Vis Sci* 2009, **50:**4360–4367.
59. Gonzales AL, Paikai A, Maeng D: **Interplay of Retinal and Choroidal Vasculatures in Ocular Health and Disease.** *Adv Exp Med Biol* 2025, **1468:**459–463.
60. Kanow MA, Giarmarco MM, Jankowski CS, Tsantilas K, Engel AL, Du J, Linton JD, Farnsworth CC, Sloat SR, Rountree A, et al: **Biochemical adaptations of the retina and retinal pigment epithelium support a metabolic ecosystem in the vertebrate eye.** *Elife* 2017, **6**.

Figure legends:

Figure 1: Systemic loss of ACOX1 decreased total retinal DHA levels. Fatty acid concentration in retinas (**A**), eyecup (RPE, choroid, sclera) (**B**) were measured in littermate *Acox1*$^{-/-}$ (knockout) and *Acox1*$^{+/+}$(wild-type) mice (n=17-18 mice per group). Statistical analysis was performed on the absolute concentration values (nmol/g) using Welch's *t*-tests. * $p < 0.05$, ** $p < 0.01$, *** $p < 0.001$. Orange: increased fatty acids; blue: decreased fatty acids; black: not significantly changed. Retinal fatty acid profile (presented in Mol%) was previously reported in Boeck et al, *J Adv Res*. 2025 Dec:78:667-680.

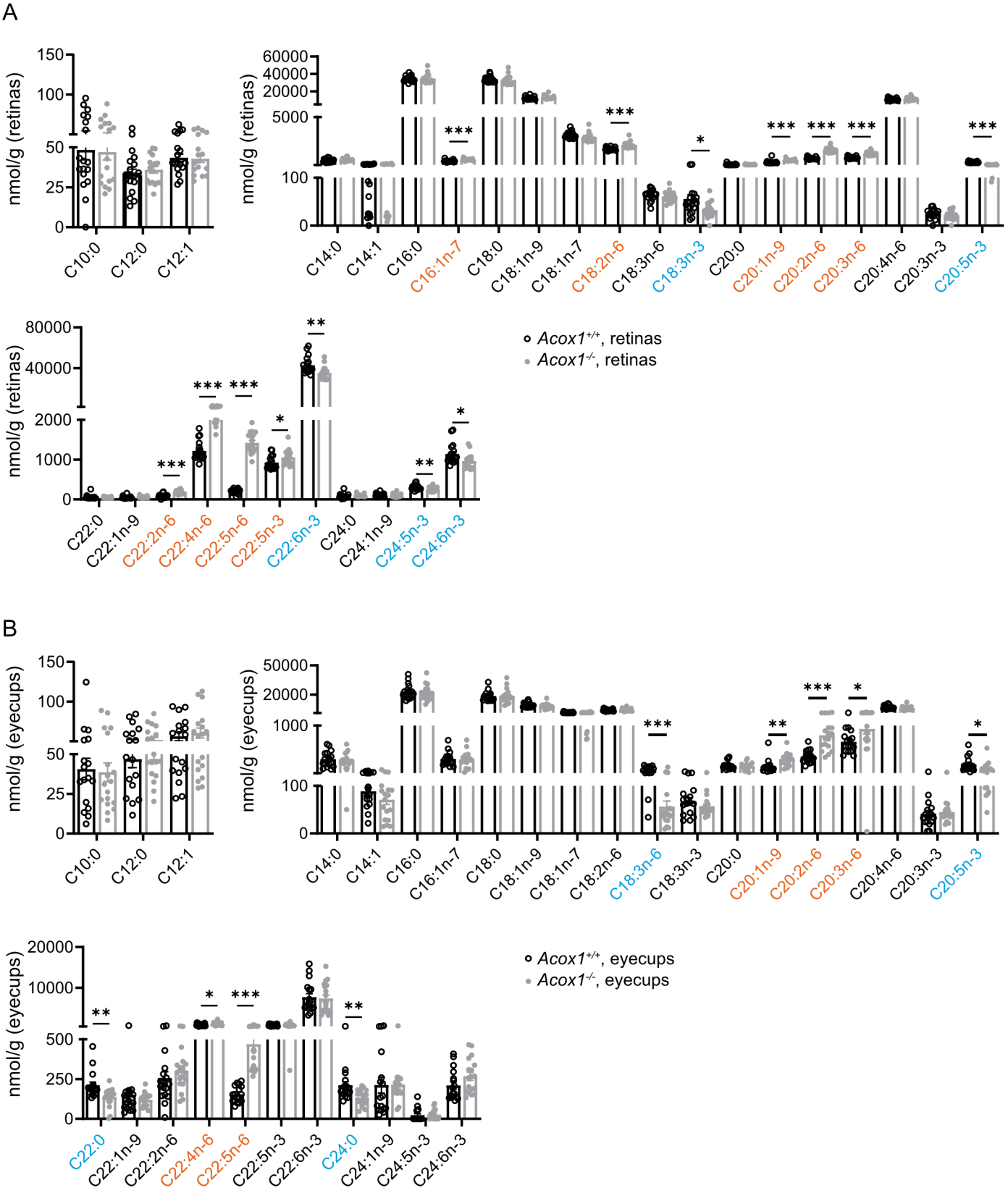
Figure 2: Rod peroxisomal ACOX1 controlled total retinal DHA levels. (**A**) Protein levels of ACOX1 in retinas from *Rho-iCre:Acox1*$^{fl/fl}$ mice were examined with western blot. *Cre+* mice were compared with littermate *Cre-* mice. ACOX1 was displayed as two bands (upper, newly synthesized; lower, the processed form). The band intensity of ACOX1 was normalized to those of internal control beta-ACTIN. n=4 mice per group. Normality (quantile-quantile plot) and F-test was first conducted, unpaired t test. ** $p < 0.01$. Fatty acid concentration in retinas (**B**), eyecup (RPE, choroid and sclera complex) (**C**) were measured in littermate *Cre+* vs. *Cre- Rho-iCre:Acox1*$^{fl/fl}$ mice (n=6 mice per group). Blue: decreased fatty acids; black: not significantly changed. Statistical analysis was performed on the absolute concentration values (nmol/g) using Welch's *t*-tests. * $p < 0.05$, ** $p < 0.01$.

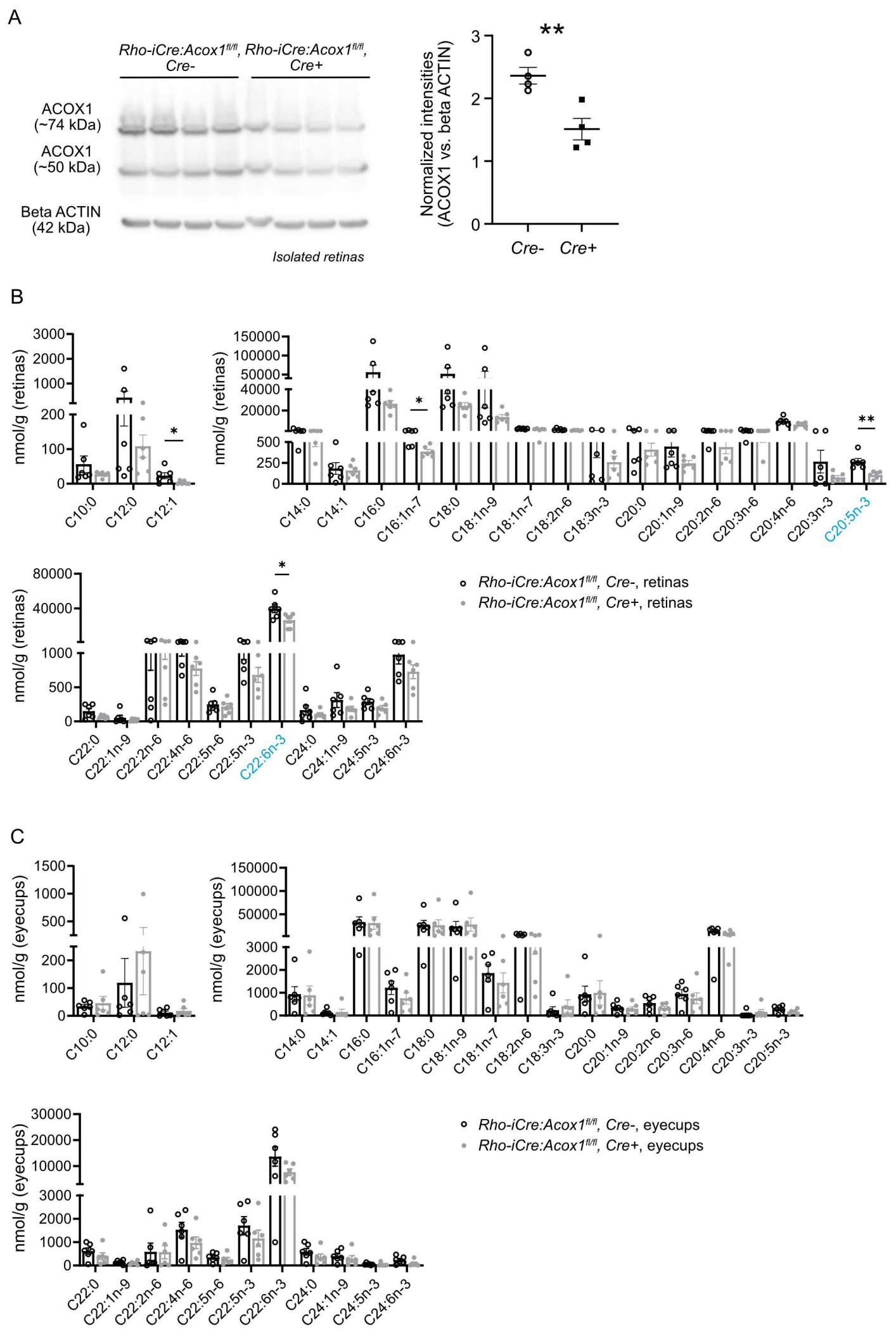
Figure 3: RPE loss of peroxisomal ACOX1 did not significantly alter fatty acid profiles in retinas and eyecups. (**A**) Protein levels of ACOX1 in RPE from *Best1Cre:Acox1*$^{fl/fl}$ mice were examined with western blot. *Cre+* mice were compared with littermate *Cre-* mice. n=4 mice per group. Normality (quantile-quantile plot) and F-test was first conducted, unpaired t test. *** $p < 0.001$. Fatty acid concentration in retinas (**B**), eyecup (RPE, choroid, sclera) (**C**) were measured in littermate *Cre+* vs. *Cre- Best1Cre:Acox1*$^{fl/fl}$ mice (n=3-6 mice per group). Black: not significantly changed. Statistical analysis was performed on the absolute concentration values (nmol/g) using Welch's *t*-tests.

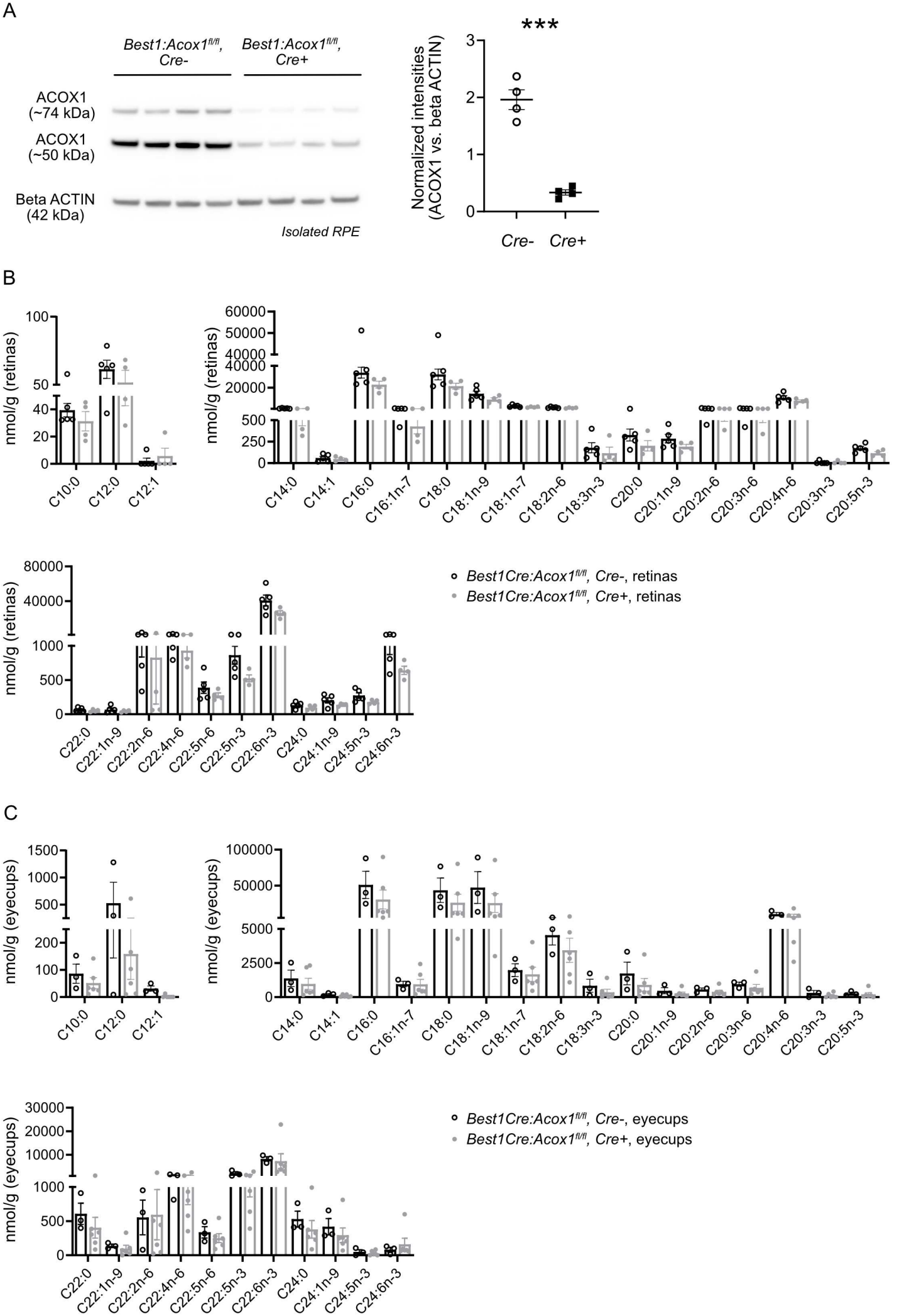
Figure 4: Loss of ACOX1 in rod photoreceptors caused defects in neural retinal signaling. (**A**) Average ERG plots were generated using average signals from the eyes in each group at selected intensities (0.001, 0.064, 2, 8, 16, 65 cd·s/m², Celeris ERG). (**B**) Rod ERG signals of *Cre+ Rho-iCre:Acox1*$^{fl/fl}$ mice were compared with littermate *Cre- Rho-iCre:Acox1*$^{fl/fl}$ controls at P30. *a*-wave, rod photoreceptors, *b*-wave, rod bipolar cells. n=14-30 eyes per group. The amplitude and sensitivity of a-waves were estimated by fitting the free parameters in a model of the biochemical processes involved in the activation of phototransduction. The amplitude and sensitivity of second-order neurons, principally bipolar cells, was measured by subtracting the mathematical model of photoreceptor responses from the intact ERG waveform and fitting the Naka-Rushton equation to the response vs. intensity relationship of the resulting waveform. (**C**) Rod ERG signals of *Cre+ Rho-iCre:Acox1*$^{fl/fl}$ mice were compared with *Cre+ Rho-iCre only* non-floxed controls at P30. n=30 eyes per group. ERG data were presented as the log change

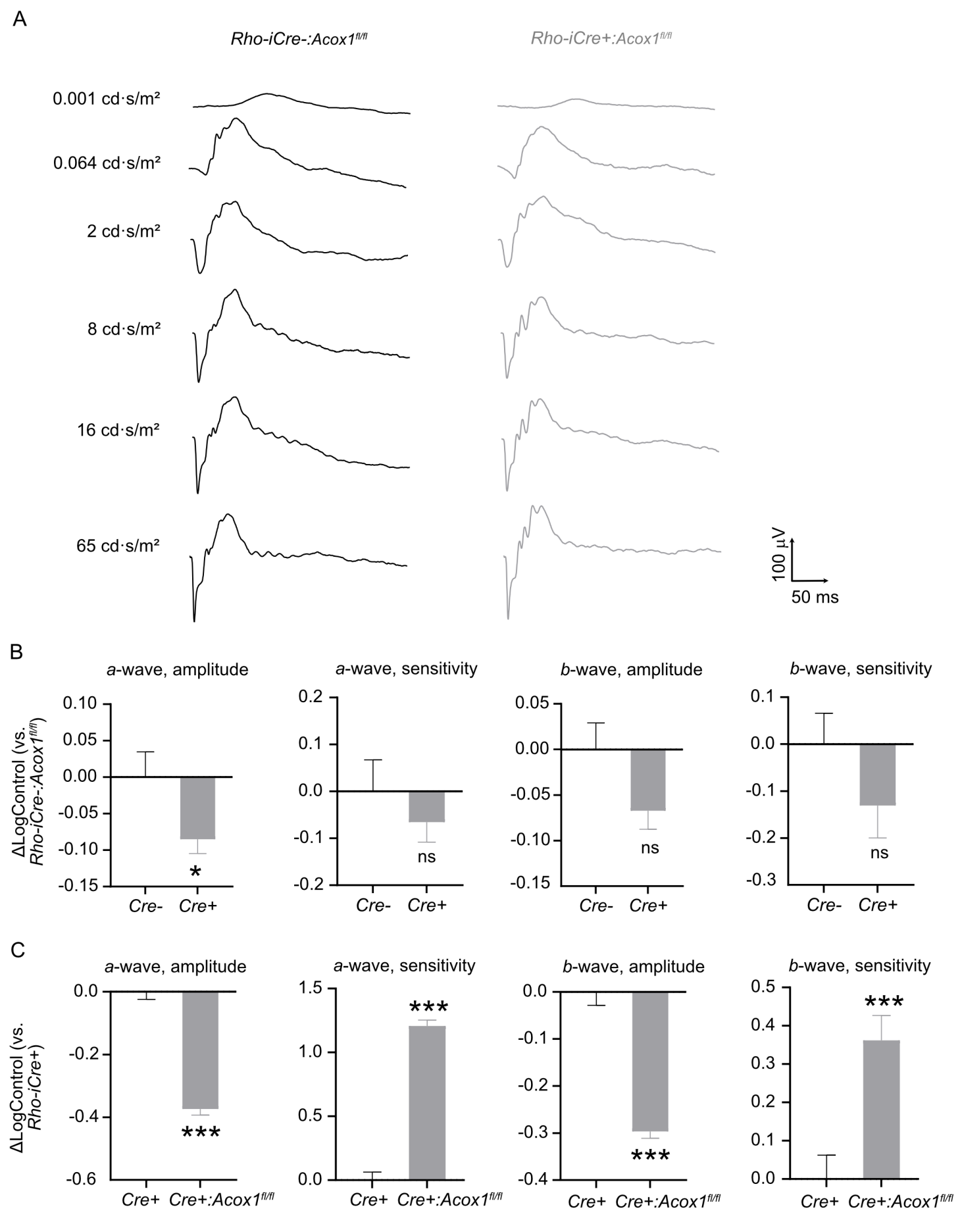
from control: negative value means decreased signals, positive value means increased signals. Normality (quantile-quantile plot) and F-test was first conducted, unpaired t-test or Mann-Whitney test was used to compare the groups. * $p < 0.05$, *** $p < 0.001$, ns, not significant.

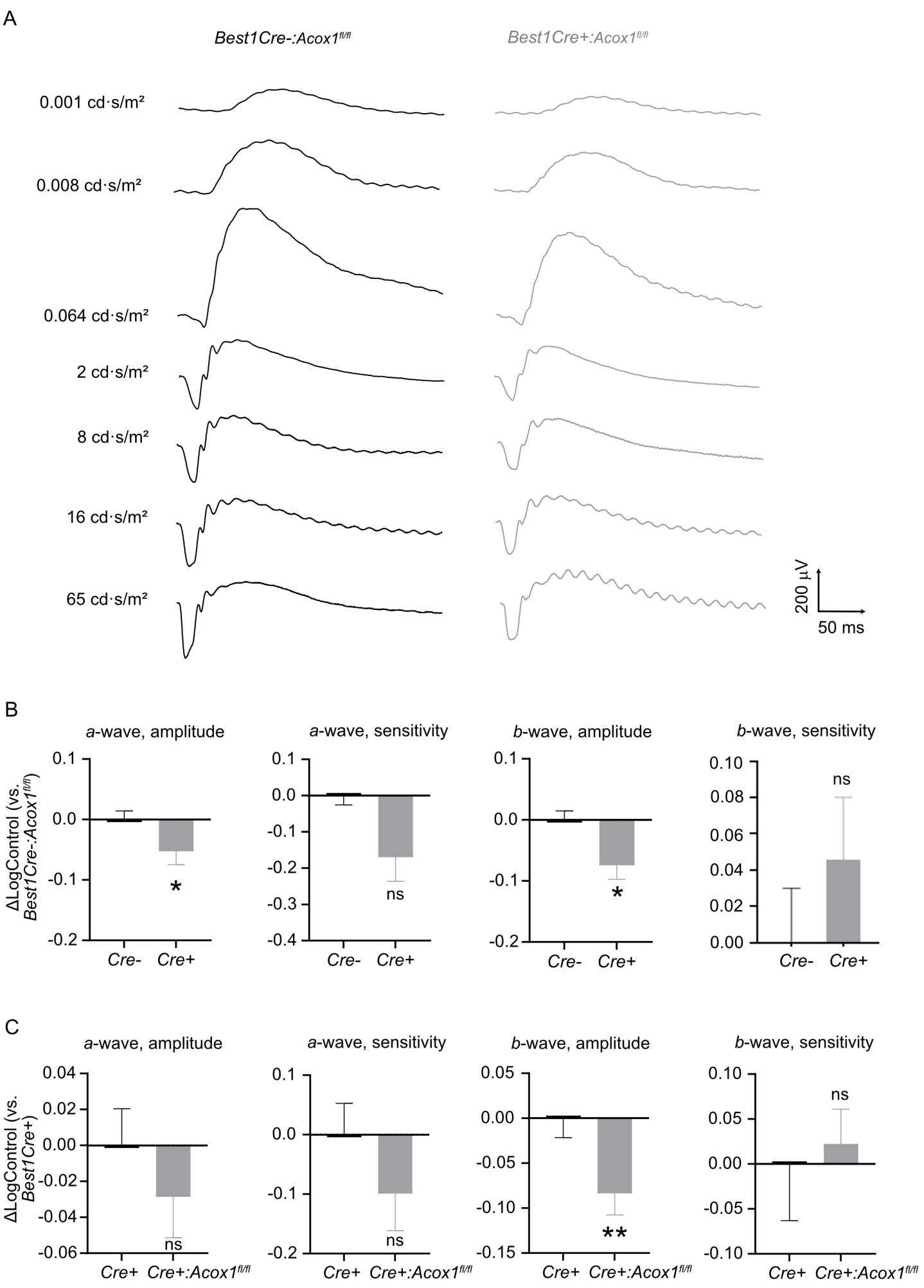
Figure 5: Loss of *Acox1* in RPE cells caused defects in neural retinal signaling. (**A**) Average ERG plots were generated using average signals from the eyes in each group at selected intensities (0.001, 0.008, 0.064, 2, 8, 16, 65 cd·s/m², Espion e^2 ERG). (**B**) Rod ERG signals of *Cre+ Best1Cre:Acox1$^{fl/fl}$* mice were compared with littermate *Cre- Best1Cre:Acox1$^{fl/fl}$* controls at P30. n=28-34 eyes per group. (**C**) Rod ERG signals of *Cre+ Best1Cre:Acox1$^{fl/fl}$* mice were compared with *Cre+ Best1Cre only* non-floxed controls at P30. n=19-34 eyes per group. The amplitude and sensitivity of a-waves were estimated by fitting the free parameters in a model of the biochemical processes involved in the activation of phototransduction. The amplitude and sensitivity of second-order neurons, principally bipolar cells, was measured by subtracting the mathematical model of photoreceptor responses from the intact ERG waveform and fitting the Naka-Rushton equation to the response vs. intensity relationship of the resulting waveform. ERG data were presented as the log change from control: negative value means decreased signals, positive value means increased signals. Normality (quantile-quantile plot) and F-test was first conducted, unpaired t-test or Mann-Whitney test was used to compare the groups. * $p < 0.05$, ** $p < 0.01$, ns, not significant.


A
nmol/g (retinas)
C10:0
C12:0
C12:1
C14:0
C14:1
C16:0
C16:1n-7
C18:0
C18:1n-9
C18:1n-7
C18:2n-6
C18:3n-6
C18:3n-3
C20:0
C20:1n-9
C20:2n-6
C20:3n-6
C20:4n-6
C20:3n-3
C20:5n-3
C22:0
C22:1n-9
C22:2n-6
C22:4n-6
C22:5n-6
C22:5n-3
C22:6n-3
C24:0
C24:1n-9
C24:5n-3
C24:6n-3
Acox1+/+, retinas
Acox1-/-, retinas
B
nmol/g (eyecups)
Acox1+/+, eyecups
Acox1-/-, eyecups


A
Rho-iCre:Acox1fl/fl, Cre-
Rho-iCre:Acox1fl/fl, Cre+
ACOX1 (~74 kDa)
ACOX1 (~50 kDa)
Beta ACTIN (42 kDa)
Isolated retinas
Normalized intensities (ACOX1 vs. beta ACTIN)
Cre-
Cre+
B
nmol/g (retinas)
C10:0
C12:0
C12:1
C14:0
C14:1
C16:0
C16:1n-7
C18:0
C18:1n-9
C18:1n-7
C18:2n-6
C18:3n-3
C20:0
C20:1n-9
C20:2n-6
C20:3n-6
C20:4n-6
C20:3n-3
C20:5n-3
C22:0
C22:1n-9
C22:2n-6
C22:4n-6
C22:5n-6
C22:5n-3
C22:6n-3
C24:0
C24:1n-9
C24:5n-3
C24:6n-3
Rho-iCre:Acox1fl/fl, Cre-, retinas
Rho-iCre:Acox1fl/fl, Cre+, retinas
C
nmol/g (eyecups)
Rho-iCre:Acox1fl/fl, Cre-, eyecups
Rho-iCre:Acox1fl/fl, Cre+, eyecups


A
Best1:Acox1fl/fl, Cre-
Best1:Acox1fl/fl, Cre+
ACOX1 (~74 kDa)
ACOX1 (~50 kDa)
Beta ACTIN (42 kDa)
Isolated RPE
***
Normalized intensities (ACOX1 vs. beta ACTIN)
Cre-
Cre+
B
nmol/g (retinas)
C10:0
C12:0
C12:1
C14:0
C14:1
C16:0
C16:1n-7
C18:0
C18:1n-9
C18:1n-7
C18:2n-6
C18:3n-3
C20:0
C20:1n-9
C20:2n-6
C20:3n-6
C20:4n-6
C20:3n-3
C20:5n-3
C22:0
C22:1n-9
C22:2n-6
C22:4n-6
C22:5n-6
C22:5n-3
C22:6n-3
C24:0
C24:1n-9
C24:5n-3
C24:6n-3
Best1Cre:Acox1fl/fl, Cre-, retinas
Best1Cre:Acox1fl/fl, Cre+, retinas
C
nmol/g (eyecups)
Best1Cre:Acox1fl/fl, Cre-, eyecups
Best1Cre:Acox1fl/fl, Cre+, eyecups


A
Rho-iCre-:Acox1fl/fl
Rho-iCre+:Acox1fl/fl
0.001 cd·s/m²
0.064 cd·s/m²
2 cd·s/m²
8 cd·s/m²
16 cd·s/m²
65 cd·s/m²
100 µV
50 ms
B
a-wave, amplitude
a-wave, sensitivity
b-wave, amplitude
b-wave, sensitivity
ΔLogControl (vs. Rho-iCre-:Acox1fl/fl)
0.10
0.05
0.00
-0.05
-0.10
-0.15
0.2
0.1
0.0
-0.1
-0.2
0.05
0.00
-0.05
-0.10
-0.15
0.1
0.0
-0.1
-0.2
-0.3
*
ns
ns
ns
Cre-
Cre+
C
a-wave, amplitude
a-wave, sensitivity
b-wave, amplitude
b-wave, sensitivity
ΔLogControl (vs. Rho-iCre+)
0.0
-0.2
-0.4
-0.6
1.5
1.0
0.5
0.0
0.0
-0.1
-0.2
-0.3
-0.4
0.5
0.4
0.3
0.2
0.1
0.0
***
***
***
***
Cre+
Cre+:Acox1fl/fl


A
Best1Cre-:Acox1fl/fl
Best1Cre+:Acox1fl/fl
0.001 cd·s/m²
0.008 cd·s/m²
0.064 cd·s/m²
2 cd·s/m²
8 cd·s/m²
16 cd·s/m²
65 cd·s/m²
200 µV
50 ms
B
a-wave, amplitude
a-wave, sensitivity
b-wave, amplitude
b-wave, sensitivity
ΔLogControl (vs. Best1Cre-:Acox1fl/fl)
Cre-
Cre+
*
ns
*
ns
C
a-wave, amplitude
a-wave, sensitivity
b-wave, amplitude
b-wave, sensitivity
ΔLogControl (vs. Best1Cre+)
Cre+
Cre+:Acox1fl/fl
ns
ns
**
ns

Supplementary Files

This is a list of supplementary files associated with this preprint. Click to download.

- SupplementalfiguresS1S3.docx
- SupplementalTable1fattyacidprofile.xlsx
- SupplementalMaterialWesternblotwholegel.docx